# Conflict Free Trajectory Optimisation with Target Tracking and Conformance Monitoring

Santi Vilardaga[1] and Xavier Prats[2]
*Technical University of Catalonia - Barcelona Tech, Catalonia (Spain)*

Pengfei (Phil) Duan[3] and Maarten Uijt de Haag[4]
*Ohio University, Athens, Ohio (United States)*

**This paper proposes an optimisation framework that computes conflict free optimal trajectories in dense terminal airspace, while continuously monitoring trajectory conformance in an effort to improve predictability. The objective is to allow, as much as possible, continuous vertical trajectory profiles without impacting negatively on airspace capacity. Given ADS-B (Automatic Dependent Surveillance - Broadcast) intent information, we predict the future state of potential intruder aircraft and use this nominal trajectory as a constraint in the ownship trajectory optimisation process. In it, a continuous multiphase optimal control problem is solved, taking into account spatial and temporal constraints. Additionally, a linearised Kalman filter keeps track of the target by estimating the deviations of its actual trajectory from its nominal trajectory, issuing a warning when an appropriate threshold is exceeded. This may be due to unexpected events, biases in the performance and weather models, wrong parameter assumptions, etc. An illustrative example is given, based on a computer simulation of two hypothetical trajectories in the Barcelona terminal manoeuvring area. The results show how this framework resolves the problem of uncertainties in the trajectory predictions and results in a more efficient conflict resolution.**

---

[1] PhD Candidate. Lecturer. Telecom and Aeropsace Engineering School of Castelldefels. Esteve Terradas, 5. Castelldefels, Catalonia (Spain).
[2] Professor. Telecom and Aeropsace Engineering School of Castelldefels. Esteve Terradas, 5. Castelldefels, Catalonia (Spain).
[3] PhD Candidate. Lecturer. Avionics Engineering Center, School of EECS, Ohio University, 208 Stocker Center, Athens, OH 45701 (United States).
[4] Edmund K. Cheng Professor. Avionics Engineering Center, School of EECS, Ohio University, 208 Stocker Center, Athens, OH 45701 (United States).

**Nomenclature**

| | |
|---|---|
| $\gamma$ | Aerodynamic flight path angle |
| $\phi$ | Bank angle |
| $\chi$ | Heading angle |
| $\pi$ | Throttle setting |
| $CI$ | Cost Index |
| $D$ | Aerodynamic Drag |
| $e$ | East coordinate |
| $FF$ | Fuel Flow |
| $g$ | Gravity acceleration |
| $h$ | Geometric altitude |
| $m$ | Mass of the aircraft |
| $n$ | North coordinate |
| $n_z$ | Vertical load factor |
| $s$ | Along path distance |
| $S_h$ | Required horizontal separation between aircraft |
| $S_v$ | Required vertical separation between aircraft |
| $T$ | Aircraft thrust |
| $v$ | True airspeed |
| $V_{CAS}$ | Calibrated airspeed |
| $V_{MCA}$ | Minimum aircraft control speed in the air |
| $V_{MO}$ | Maximum aircraft operating speed |
| $W_e$ | East wind component |

$W_n$ North wind component

## I. Introduction

Timely and accurate aircraft trajectory predictability is paramount for efficient and safe operations in air traffic management (ATM). Continuous Climb Operations (CCO), Continuous Cruise Climbs (CCC), and Continuous Descent Operations (CDO) have demonstrated good fuel reduction in specific phases of the flight, but are greatly dependent on multiple characteristics of each aircraft (such as aircraft performance, mass or operating procedures) and meteorological conditions. This results in a great variety of individually *optimal* vertical and speed profiles that, in combination with the lack of information-sharing between airspace users, complicates the task of predicting aircraft future states and traffic separation, ultimately impacting negatively on airspace capacity [1].

Currently, aircraft separation is mainly handled, at a strategic level, by spacing air navigation procedures (in the horizontal or vertical domain) in order to minimise potential airborne encounters; and, at a tactical level, by giving open instructions to individual aircraft to remove any remaining conflict. However, this usually leads to inefficient operations, preventing the aircraft flying optimised trajectories (i.e., CDO and CCO), increasing fuel and pollutant emissions and producing a larger noise impact in the vicinity of the airport. To address these negative aspects, the SESAR and NextGen programmes define the concept of Trajectory Based Operations (TBO), which relies on pre-established conflict-free efficient trajectories. For example, Ref. [2] proposes the implementation of applicable speed and heading advisories to current operations to resolve conflicts during cruise phase using TBO operational concept. Ref. [3] assesses the application of TBO air-ground synchronisation concepts with current technologies and its predictability issues. Finally, Ref. [4] presents the application of CDO within high traffic operations with the use of time advisories, or required time of arrivals (RTA) at given fixes. The impact on fuel consumption using RTAs versus continuous operations (CDO and CCO) in the Terminal Manoeuvring Areas (TMAs) has been assessed, for instance, in Ref. [5].

One requirement for efficient flow of air traffic is the accurate knowledge of aircraft (ownship and intruders) positions, velocity and adequate prediction of future aircraft movements. Without

accurate information, maintaining safe separation between aircraft requires much more conservative, and therefore less efficient, methods [6, 7]. Moreover, a large scale implementation of these optimised trajectories (i.e., not only for a small set of aircraft but for all those in a dense and complex TMA) remains an issue that will obviously require more levels of automation. In this regard, the concept of aircraft self-separation is seen as a promising solution. The recent iFly project(footnote: http://ifly.nlr.nl/) claims this concept may safely accommodate up to six times the en-route traffic demand of 2005 [8]. The distributed nature of this solution provides localised case-by-case efficient near- and mid-term conflict resolution (from minutes to tens of minutes), even if the long-term (hours) efficiency can be included in combination with ground assistance as depicted in Ref. [9]. This will also result in lower ground infrastructure complexity and reduced associated costs compared to a fully centralised solution.

The problem described in the previous paragraphs is of a complex nature, requiring advances in trajectory optimisation, trajectory prediction and conformance monitoring. The literature on the three individual challenges is extensive. Individual trajectory optimisation can be approached from a variety of models and methods, from sampling-based path planning (e.g., Dijkstra, $A^*$, $RRT^*$ [10]), to stochastic optimisation (e.g., Genetic Algorithms, Causal Models [11]), to a continuous and constrained optimal control problem [12–15]. Advances on the latter are presented in this paper as a complete generic optimisation framework. An extensive review on trajectory prediction methods is presented in Ref. [16]. This paper presents advances on this field by using optimisation methods as oposed to other conventional approaches, which usually consist of the integration of the equations of motion over time, assuming a given set of aircraft intents. Finally, on conformance monitoring most of the research efforts have been put into detecting anomalies and deviations from a reference path [6, 17–21]. However, even if these present methods to trigger an alarm at the earliest convenience, to the best of our knowledge, a complete end-to-end study that includes continuous conformance monitoring with online implementation of optimal corrective actions throughout a whole flight phase has not been previously presented.

This paper is organised as follows. Section II describes the applicable assumptions and cooperation modes in the concept of operations. Section III lays out the dynamic model of the aircraft

and the problem formulation, including the flight phases, operational constraints and separation assurance. Section IV describes the conformance monitoring implementation. Section V describes the scenarios and results that have been obtained. Finally, section VI presents the authors' conclusions.

## II. Concept of operations

In a terminal manoeuvring area (TMA or TRACON), where a high density of traffic struggles to safely and efficiently navigate towards a destination, cooperation between all involved actors is an important issue to address. This becomes even more important in a future scenario, where the aircraft themselves are responsible for maintaining separation, thus delegating ATC responsibilities to the pilot through the use of airborne separation assurance systems (ASAS) [22]. The major driver for effective cooperation is the amount of information that is shared amongst airspace users. From everything to nothing, three information sharing cases are considered:

**Case A: Fully-cooperative**

An ideal scenario would assume a fully cooperative situation where trajectory optimisation benefits from knowledge of intruder aircraft performance data and intents. Some implementations of this case assume centralised computation of all traffic optimal trajectories [2]. Another strategy would be to delegate the computation of optimal trajectories and conflict resolution to the cockpit. In that case, each aircraft calculates its own optimal trajectory taking into account the prediction of other traffic future states and then enters in a collaborative decision making process with the potential conflicting aircraft to find the overall best conflict resolution. Ref. [5] concludes that this coordinated distributed strategy can render very efficient results.

**Case B: Semi-cooperative**

Nowadays, airlines are very wary on providing sensitive information to other airspace users (mainly aircraft mass and cost index strategy). Hence, another (less cooperative) solution is to use a flight plan or flight intent information to predict other aircraft trajectories, with the assumptions of unknown aircraft parameters. This solution relies on ADS-B/C data or the implementation of cooperative methodologies such as AIDL (Aircraft Intent Description

Language) [23] and SWIM (System Wide Information Management) [24]. In that case, a conflicted user can perform ownship optimisation separating from a prediction of other traffic future states. Again, a collaborative decision making process might be required, in this case to determine which aircraft has the responsibility to keep the required separation from other traffic.

**Case C: Non-cooperative**

The third case assumes there is (almost) no direct form of information sharing between aircraft. In this case, only historical position data (as coming from either ADS-B, if available, or from primary radar tracks) can be used to predict potential intruder future states [25]. The resulting huge prediction uncertainty adds complexity to the deconflicting problem. No collaborative decision making process is required here as it is assumed that the intruder might suffer from technical problems (unavailability of the on-board transceiver) or is unwilling to cooperate.

The collaborative decision making process mentioned for Case A and Case B can be tackled at two different levels. On the one hand, aircraft could be required to meet strategically externally imposed constraints (e.g., in form of time or speed advisories) throughout the flight path that would resolve the conflict (an example of this is presented in Ref. [5]). On the other hand, it could be effectively decided that the deviation responsibility is established upon one aircraft (the ownship), who should deviate from the other traffic in the problem (intruder/s). This decision might be done in real-time depending on aircraft parameters (e.g., weight or speed), or network effects (impact to future potential conflicts) or, alternatively, through pre-established convention (pre-agreed between airports, routes, right-of-way, etc).

This paper explores a possible implementation and the implications of the semi-cooperative case (Case B), where an ownship (pre-established by strategic decision) must calculate a conflict-free trajectory away from other traffic. The aircraft performance data can easily be inferred, either assuming similarities with aircraft in the ownship airline's fleet (i.e., same aircraft model), using openly available aircraft dynamic models (e.g., BADA[(footnote: Eurocontrol's Base of Aircraft Data)]), or through the said future collaboration frameworks. Similarly, the flight plan of other traffic is quite straightforward to fetch. However, parameters such as the take-off mass or the cost index strategy

will most surely remain unknown to other users in the airspace. Therefore, this paper presents a methodology where an ownship predicts intruding traffic trajectories with the said assumptions, then recalculates its own optimal trajectory avoiding the potential conflicts and continuously monitoring the validity of the predictions to account for the uncertainties in the model and assumptions. This deconfliction aims at tactical traffic separation either because strategic deconfliction is non-existent, or it has failed due to unexpected events at the time of execution.

## III. Conflict-free 4D trajectory optimisation

There are multiple approaches to the computation of a trajectory that complies with a set of constraints. Some of them are described in Ref. [5]. The algorithms in this paper are based on optimal control concepts: in order to cope with the important non-linearities in the different equations, and to optimise multiple-phase complex aircraft trajectories, we convert the infinite-dimensional original problem into a finite-dimensional non-linear programming (NLP) problem with a finite set of decision variables in the time interval $[t_0, t_f]$ [12]. This approach allows the definition of complex trajectories while complying with the set of dynamic equations, the given multi-phase constraints and minimising a cost functional, thus providing an accurate and flexible optimal trajectory framework.

### A. Problem formulation

Let $\boldsymbol{x}(t) \in \mathbb{R}^{n_x}$ be the state vector describing the trajectory of the aircraft at time $t$ and $\boldsymbol{u}(t) \in \mathbb{R}^{n_u}$ the control vector that leads to a specific trajectory.

Our goal is to find the best trajectory that minimises the following cost functional:

$$J = \int_{t_0}^{t_f} [FF(\boldsymbol{x}, \boldsymbol{u}) + CI] \, \mathrm{d}t. \tag{1}$$

The Cost Index ($CI$) scalar relates the cost of time to the cost of fuel (computed from the fuel flow; $FF$) and takes into account different airline policies. Moreover, the value of $t_f$ is a decision variable itself and will be fixed by the optimisation algorithm.

We have formulated an optimal control problem, the solution to which minimises the objective defined in Eq. (1) with the state and control vectors defined as follows (unknowns of the problem):

$$\begin{aligned} \boldsymbol{x} &= [\ v\ \ \gamma\ \ \chi\ \ e\ \ n\ \ h\ \ m\ ] \\ \boldsymbol{u} &= [\ n_z\ \ \phi\ \ \pi\ ]. \end{aligned} \tag{2}$$

In order to guarantee that the optimisation process results in a feasible and acceptable trajectory, several constraints are considered.

The first constraint models the dynamics of the system expressed by non-linear differential equations. In this paper, a point-mass representation of the aircraft is used, where forces apply at its centre of gravity. A situation with benign and constant winds in a flat non-rotating earth has been assumed. The equations of motion are written as follows [26]:

$$\begin{aligned} \frac{\mathrm{d}v}{\mathrm{d}t} &= \dot{v} &&= \frac{1}{m}(T - D - mg\sin\gamma) \\ \frac{\mathrm{d}\gamma}{\mathrm{d}t} &= \dot{\gamma} &&= \frac{g}{v}(n_z\cos\phi - \cos\gamma) \\ \frac{\mathrm{d}\chi}{\mathrm{d}t} &= \dot{\chi} &&= \frac{g}{v}\frac{\sin\phi}{\cos\gamma}n_z \\ \frac{\mathrm{d}e}{\mathrm{d}t} &= \dot{e} &&= v\cos\gamma\sin\chi + W_e \\ \frac{\mathrm{d}n}{\mathrm{d}t} &= \dot{n} &&= v\cos\gamma\cos\chi + W_n \\ \frac{\mathrm{d}h}{\mathrm{d}t} &= \dot{h} &&= v\sin\gamma \\ \frac{\mathrm{d}m}{\mathrm{d}t} &= \dot{m} &&= -FF \end{aligned} \tag{3}$$

To model the atmosphere, a set of polynomial approximations has been implemented to define the density $\rho$, pressure $p$ and temperature $\tau$ magnitude as functions of the altitude and geographic location. The polynomials are populated using weather forecast from

GRIB(footnote: General Regularly-distributed Information in Binary form: format to store and share weather data.) files.

All aerodynamic and engine parameters are represented by continuous polynomials, that ensure continuity for the first and second derivatives as it is required for the numerical solvers used here. Aerodynamic Lift ($L$) and Drag ($D$) forces are modelled considering air compressibility effects, which cannot be neglected for nominal cruising speeds of typical commercial aircraft (between M.78 and M.82 approximately). Tabulated aircraft aerodynamic data has been obtained from Airbus Performance Engineers Program (PEP) software suite, which provided us with accurate (and certified) values for aerodynamic drag and engine performance for different flight conditions. More details about the specific implementation are found in Refs. [5, 27].

Besides the equations of motion described above, the problem is further constrained by additional equations that take into account several operational restrictions as described in table 1 (where $V_{MCA}$ is the minimum control airspeed airborne; while $V_{MO}$ is the maximum speed in operations).

**Table 1 Constraints in the optimal control problem**

| Constraint | Definition |
|---|---|
| Operating airspeeds | $V_{MCA} \leq v_{CAS}(t) \leq V_{MO}$ |
| No deceleration allowed | $\dot{v}_{CAS}(t) \geq 0$ |
| No descent allowed | $\dot{h}(t) \geq 0$ |
| Minimum climb gradient | $h(t) \geq 0.033 s(t)$ |
| Load factor | $0.85 \leq n_z(t) \leq 1.15$ |
| Bank angle | $-25^\circ \leq \phi(t) \leq 25^\circ$ |

### B. Separation assurance

Finally, requiring separation from other traffic is another constraint in the problem. Figure 1 depicts a block diagram of the proposed methodology, involving an aircraft (the ownship) separating from surrounding traffic (one intruder).

To generate a trajectory that deviates from an intruder, the ownship collects the following required data from the other aircraft:

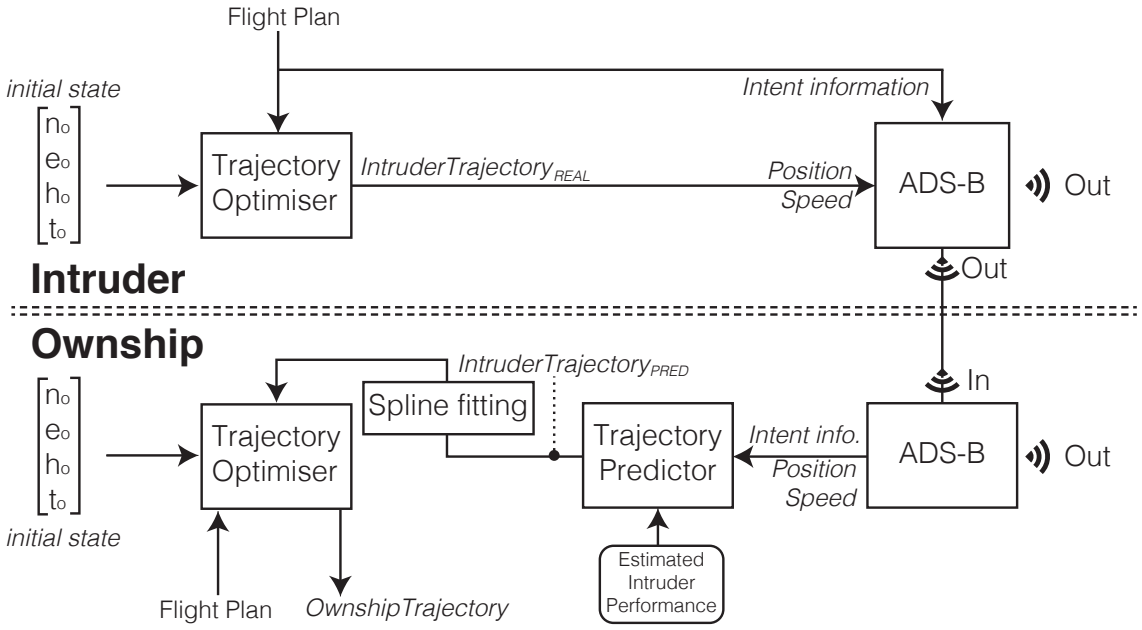


**Fig. 1 Block diagram of the aircraft separation methodology proposed in this paper**

**Updated position and velocity** To be used as the initial state for the prediction algorithm.

**Flight plan or short-term intents** The next couple of waypoints (two or three suffice) as these represent the expected route that the aircraft will follow. The more information coded in these intents, the more accurate the prediction will be. In this paper we have assumed geographical information only (latitude, longitude mainly, and altitude restrictions if provided), but time and velocity information as calculated in real time by the flight management system would render the prediction more accurate.

**Type of aircraft** To be used to select the performance model and parameters (i.e., nominal values for drag coefficients, mass, etc.)

This information could come from a fully implemented ADS-B protocol (as specified in [28]) or other transmission protocols and frameworks such as TIS-B or SWIM. In this paper we have assumed ADS-B as the data exchange technology (and message format), where the above-mentioned required information is directly accessible, or easily extrapolated, from the identification message, position message and intent message. This information is then used to predict the intruder future states (i.e., from the current intruder's position and velocity, following the flight intents, using the aircraft

type performance) and calculate the ownship optimal trajectory that keeps the required separation. The separation strategy described in this section is easily extrapolated to multiple conflicts. The following subsections describe the different parts of the methodology in further detail.

*1. Intruder trajectory prediction*

Prediction methods in the literature are usually based on the numerical integration of the intruder aircraft dynamics with specific assumptions required to close the degrees of freedom in the dynamic equations (e.g., in form of a fixed throttle setting, vertical speed or flight path angle) [16]. These usually lead to complex iterative (and costly) processes to adjust the controls in order to meet the aircraft intents. Instead of fixing such controls (and adjust them when we see that we do not comply with a specific constraint), we propose to use an optimisation method, which will modulate the controls as required in order to comply with the set of constraints.

This method allows for more complex predictions and can potentially provide more accurate results when many restrictions apply to a trajectory. Specially, when a flight plan is available that follows a defined lateral route (e.g., as coming from an standard departure procedure) and when multiple constraints have to be met at one fix (e.g., altitude and time). Given the fact that more than one trajectory will be available as a solution to the prediction problem (e.g., climb first vs. accelerate first), our strategy does not just provide one of the possible trajectories that meets the constraints (the one that the given fixed controls have generated), but it provides the one that is most cost effective (assuming an optimisastion objective given by Eq. 1). Obviously, the more accurate the intents are, the better the prediction will be.

The remaining challenge is how to model this moving target in our optimisation problem as continuous and twice differentiable functions needed by the NLP solver. Our approach is to represent the state of the moving target by time-dependent polynomials. Because a trajectory can be a very complex curve, we rely on polynomial fitting to model a predicted reference trajectory [29]. Therefore, the list of 4D points coming from the predicted intruder trajectory is fit by a set of basis splines (B-splines) using the open source library *einspline*[(footnote: http://einspline.sourceforge.net/)].

A Cubic B-spline is a continuous twice-differentiable function represented by piecewise polyno-

mials of order three. As opposed to high degree polynomials, these provide an accurate curve fit and have been demonstrated to perform well with NLP optimisation [27] as they can be very smooth.

Effectively, this solution has proven to be very reliable, robust and have good performance in our simulations. Our approach is to create three splines that represent the intruder's north, east and altitude coordinates over time ($\Gamma_n(t)$, $\Gamma_e(t)$ and $\Gamma_h(t)$ respectively). At the ownship optimisation process, the algorithm will repetitively query these curves that represent the dynamic obstacle (intruder) at each time of sample ($t$).

*2. Separation volume*

Current radar separation ATC procedures in TMA specify lateral and vertical separation independently, given the big difference in dynamics between the horizontal and vertical planes, forming a cylindrical protection volume: from 2.5NM to 5NM in horizontal and 1000ft to 2000ft in vertical space, depending on technical and environment related aspects [30]. Thus, a *conflict* appears when there is a risk of an aircraft entering this protection volume unless separation action are taken. This could lead to a loss of separation and eventually to a near mid-air collision or ultimately a fatal encounter.

The cylindrical separation volume constraint can be described with the following disjunction:

$$g_h(t) \geq 0 \vee g_v(t) \geq 0 \tag{4}$$

where $g_h$ and $g_v$ are the horizontal and vertical separation constraints:

$$\begin{aligned} g_h &= \sqrt{(n(t) - \Gamma_n(t))^2 + (e(t) - \Gamma_e(t))^2} - S_h \\ g_v &= (h(t) - \Gamma_h(t)) - S_v. \end{aligned} \tag{5}$$

As stated before, NLP solvers require continuous and twice differentiable functions, and it is obvious that a cylinder does not comply with this. To solve this issue, one can reformulate Eq. (4) with continuous functions as follows [31]:

$$\lambda_h(t)g_h(t) + \lambda_v(t)g_v(t) \geq 0$$

$$\lambda_h(t) + \lambda_v(t) = 1 \tag{6}$$

$$\lambda_h(t), \lambda_v(t) \geq 0$$

where $\lambda_h$ and $\lambda_v$ are two continuous variables that, with the second and third constraints in (6), enforce the logical OR in this formulation. The nature of this formulation, however, will presumably add complexity to the solver, increasing computational times and increasing the risk of local minima.

Other strategies could bring better convergence to the algorithm with the cost of a less accurate representation of the separation volume. This would be, for example, in case of a sphere [32] or an ellipsoid [33]. These are geometrical forms that can be expressed by a single equation and, specifically to our problem, enforce separation by form of inequalities. In contrast to the current cylindrical specification, the sphere is highly inaccurate as it treats lateral and vertical separation equally and ellipsoids are also very inaccurate at the horizontal extremes (i.e., the vertical separation is soon lost when going towards the horizontal edges). However, a specific case of super-ellipsoids, the supereggs, can be parametrised in a way to form a geometrical shape very close to that of the cylindrical protection volume. Effectively, these are very similar to ellipsoids but maintain the vertical separation longer, to a steeper end. They can be represented by the following equation:

$$\left(\frac{(n(t) - \Gamma_n(t))^2 + (e(t) - \Gamma_e(t))^2}{{S_h}^2}\right)^p + \left(\frac{(h(t) - \Gamma_h(t))^2}{{S_v}^2}\right)^p \geq 1 \tag{7}$$

where $p$ is the steepness coefficient of the superegg. A higher value is closer to the representation of a cylinder but more complex for the convergence of the algorithm. In our computations, $p = 3$ has provided a good trade-off.

Although it is out of the scope of this paper to thoroughly study each strategy, we have implemented both the cylindrical disjunction described in (6) and the supereggs inequality described in (7). The first strategy, as expected, fully respects the cylindrical protection volume but the non-linear nature of it results in the optimiser falling into local minima easier. The second strategy shows

a slightly less accurate representation of the protection cylinder (i.e., the vertical separation is found to be slightly less than the required minima when the horizontal separation is at its bounds), but presents less non-linearities for the model, and thus performs very well on the optimisation engine. With an adequate choice of superegg coefficients, the inaccuracies of the superegg as compared to the cylinder have been demonstrated to be very small and, therefore, the results in this paper use this strategy.

### C. Optimisation framework

Aircraft trajectories are divided into multiple flight phases with specific performance values assigned to each phase. During the first phase of its trajectory, an aircraft will be climbing at maximum take-off thrust without the possibility of turning or making changes to the aerodynamic configuration. The phases following this initial climb are defined by the different and sequential aerodynamic changes (flaps/slats retraction). These aerodynamic configuration changes are typically executed at predefined speed steps. Besides, the departing aircraft follows a route specified by a set of vertical, lateral and speed constraints described in the published Standard Instrument Departures (SID). Additionally, such constraints may also be issued by an air traffic controller (ATCo) at a tactical level, along with one or several RTAs in a 4D trajectory scenario. In this paper, we have used these switching functions to take into consideration the changes in aerodynamic configurations, which allows the use of the phases of the optimal control problem formulation to model the ordered list of fixes defining the lateral and vertical route. With this solution, we are able to compute a full trajectory from a set of initial conditions to a set of final conditions, including one or more RTAs in the fixes along the route using a constrained multi-phase optimal control problem.

The optimisation framework described in this paper integrates different modules. The software tool has been mainly developed in C++ and General Algebraic modelling System (GAMS[footnote: http://www.gams.com]). The core part of the optimiser is written in GAMS, given the facility and robustness it provides to implement optimal control problems and the multiple NLP solver engines to which it seamlessly links. All other software modules are written in C++, including a wrapper to the core functionality. Thus, we can dynamically define and load scenarios

(described by a Flight Plan and many other problem parameters), prepare them for the optimisation and gather the results once done. The flexibility of the described framework allows for an easy implementation of different flight profiles, from completely unconstrained continuous operations, to defined standard procedures such as Noise Abatement Departure Procedures (NADP), standard instrument departures and arrivals (SID, STAR), etc. as well as any ATC constraint.

## IV. Conformance monitoring

In addition to calculating a conflict-free situation, the target traffic prediction is continuously monitored to account for uncertainties in the prediction process. The conformance monitoring methodology is depicted in figure 2 and described in the following paragraphs.

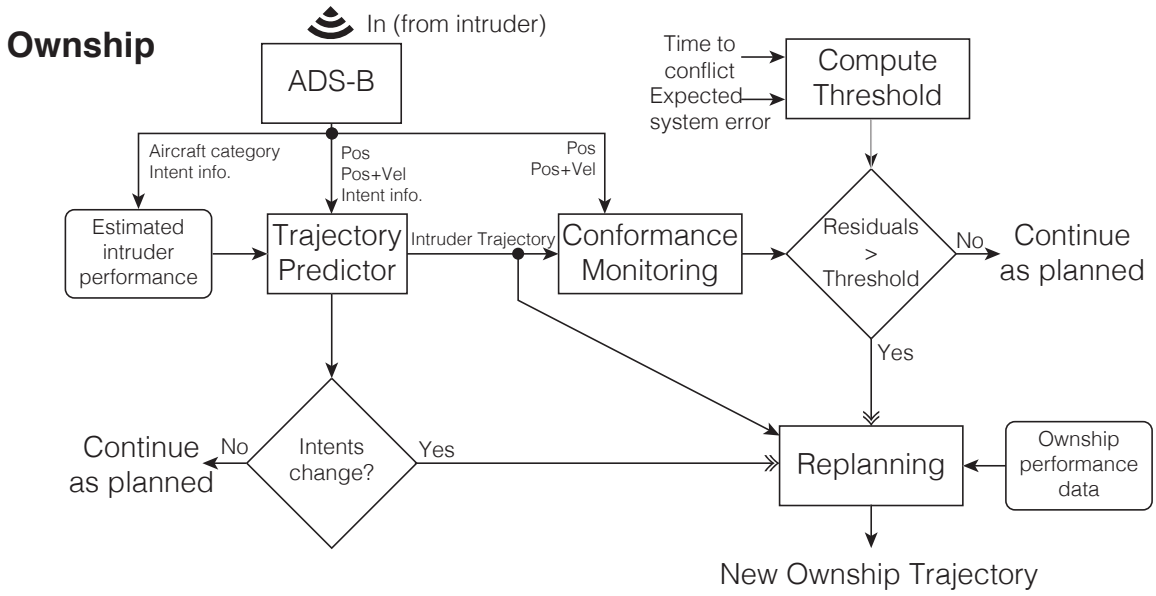


**Fig. 2 Flow chart of the proposed methodology of separation assurance with conformance monitoring.**

The method is the combination of an intruder's reference trajectory (as predicted from the ownship, detailed in the previous sections) and a target tracker based on limited information from ADS-B (i.e., position and velocity). We define a linearised Kalman filter with six states, which account for the difference in position and velocity between the predicted trajectory and the true ADS-B reports:

$$\boldsymbol{y} = [\ \Delta e\ \ \Delta n\ \ \Delta h\ \ \Delta \dot{e}\ \ \Delta \dot{n}\ \ \Delta \dot{h}\ ]^T \tag{8}$$

where $\Delta$ represents the difference of the state between actual and nominal trajectory. The measurement equation is given by:

$$\boldsymbol{z} = \boldsymbol{y} + \boldsymbol{v} \tag{9}$$

where $\boldsymbol{z}$ is the measurement and $\boldsymbol{v}$ is the measurement noise with covariance matrix $\boldsymbol{R}$. $\boldsymbol{R}$ is derived from Navigation Accuracy Category for Position (NACp) and Navigation Accuracy Category for Velocity (NACv) from ADS-B messages. The state transition equation from time epoch $k-1$ to time epoch $k$ is defined as:

$$\boldsymbol{y}_k = \boldsymbol{\Phi}_k \boldsymbol{y}_{k-1} + \boldsymbol{w}_k \tag{10}$$

where $\boldsymbol{\Phi}_k$ is the state transition matrix for a constant velocity model [34] and $\boldsymbol{w}_k$ is process noise reflecting the uncertainty in the dynamics model for the flight operation (e.g., departure in this paper) and mainly determined by unmodelled dynamics due to the aircraft's flight technical error. The covariance matrix for $\boldsymbol{w}_k$ is the state transition covariance matrix $\boldsymbol{Q}$. Note that the constant velocity model is applied to the trajectory deviation rather than the aircraft dynamic model, as it is obvious that aircraft is not flying constant velocity during departure flight phase. For the results in this paper we have assumed a time step of 1s.

The mechanisation of the filter states allows to take into account the history of the observables (ADS-B reports), reducing the noise from the position and velocity reports and the ability to perform a short-term prediction. With this method, the conformance monitoring is directly interpreted from the state variables of the filter. In other words, as opposed to a mere comparison between the state of the intruder and the predicted trajectory, the presented method allows to take into account the history of all measurements/reports from the ADS-B receiver to come up with estimates and predictions that are more accurate (lower noise) than the instantaneous reports.

The state vector is compared to a pre-defined threshold to determine whether a new prediction of the intruder's trajectory has to be calculated and, consequently, a new trajectory replan is required for the ownship. The values of the pre-defined threshold are based on typical navigation system error (NSE), flight technical error (FTE), and the aircraft dynamics. The choice of the threshold is a trade-off between minimising the possibilities of missed detection and false alarm. The threshold values used in the example in the following section are typical or conservative values for demonstration purposes. A performance analysis for the optimal choice of the threshold will be reported in future work.

## V. Numerical example

A typical conflict that is encountered within a TMA is usually due to the close proximity of two airports (like it happens for instance in the Bay Area around San Francisco airport or in the New York Area, and mostly all over Europe) or between departures and arrivals at the same airport.

### A. Scenario setup

For the purpose of this paper, we have prepared a scenario following close-to-real life operations in two airports in the Barcelona TMA. The Airbus A320, a typical twin-engine narrow-body aircraft, has been simulated in all the cases explained below. Aircraft departing Barcelona (LEBL) and Reus (LERS) airports have been considered and we have focused on two departures from each airport that create a conflict. In Reus, the current eastward departure procedure BCN1S makes a long detour to strategically deconflict departing traffic with inbound and outbound traffic of Barcelona airport (see Figure 3). In SESAR and NextGen, with the concept of TBO, these long detours may be replaced by pre-cleared 4D trajectories. Hence, in this paper we study a new, more fuel efficient, straight departure route as depicted in the same figure.

Let RES refer to the trajectory of an aircraft departing from Reus and following this new departure route and let BCN refer to the trajectory of another aircraft that departs Barcelona to the west through the GRAUS3W SID. Figure 3 shows the lateral routes as resulting from the optimiser, overlaid on the charts defined in the Spanish Aeronautical Information Publications (AIP)

[35, 36].

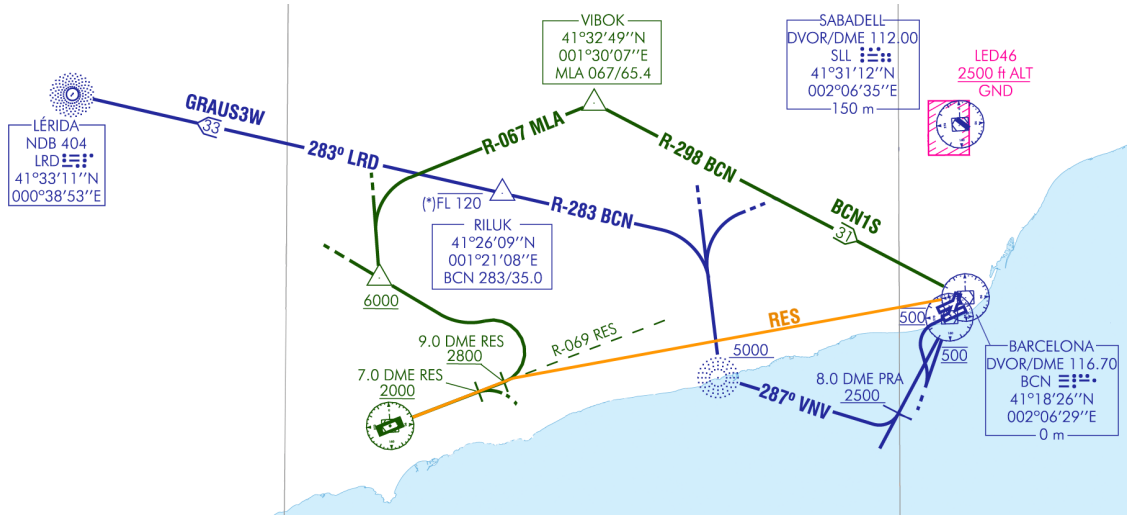


**Fig. 3 Published standard instrument departures for Barcelona (GRAUS3W, blue) and Reus (BCN1S, green) and proposed direct route (RES, orange).**

This new direct route from Reus is more likely to create conflicts with traffic in Barcelona and effectively, two aircraft departing at approximately the same time with a similar take-off mass enter in conflict soon after take-off. Therefore, some action is required to prevent the loss of separation. This situation could be estimated just before take-off, since every aircraft has a (fairly)accurate prediction of its own future states. However, due to the very limited degree of information sharing between airspace users, it is much more difficult from an external entity (e.g., another aircraft) to synthesise such accurate predictions of other traffic: sensitive data such as aircraft weight and performance data remain unknown.

To reflect this issue, we simulate the situation where the ownship (BCN) predicts the intruder (RES) trajectory and deviates from it. To demonstrate the functionality of the conformance monitor we assume that both aircraft have similar performances, but that the onwship underestimates the intruder's take-off mass (5% lower).

In this example, both aircraft are flying a departure procedure with a required navigation performance of RNP 0.3. In other words, nominally, the target aircraft should never have a lateral deviation of more than 0.6NM (two-sigma containment radius) from the nominal trajectory [37]. As a result, if the target aircraft is found to be deviating more than 0.6NM, it is likely due to an

intentional change of flight path or mismodelling of the nominal trajectory. Therefore, 0.6NM is used as the lateral position deviation threshold for monitor (a). Similarly, 250ft [38] is used as the threshold for the vertical position deviation and a conservative value of 5m/s is used for the velocity threshold. A NACp of 10 (corresponding with 95% estimated position error of 10m horizontally and 15m vertically) and NACv of 3 (corresponding with velocity error of 1m/s horizontally and 5ft/s vertically) [39] are used to define the measurement covariance matrix $\boldsymbol{R}$.

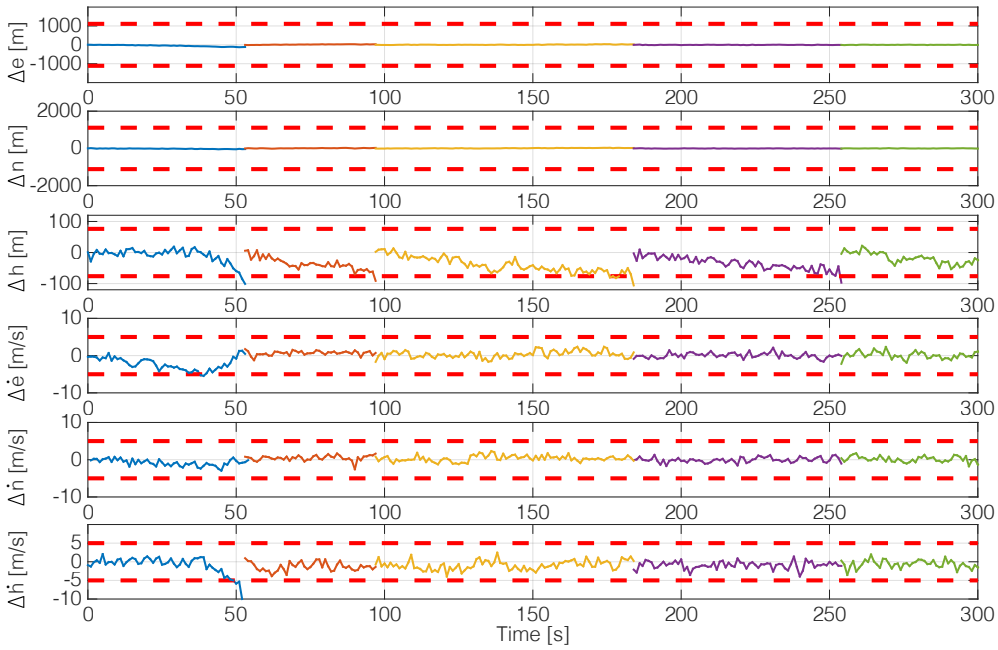


**Fig. 4 Intruder state vector deviation showing the prediction errors and the trespassing of the threshold at each replan.**

### B. Simulation results

The induced prediction errors lead to time, speed and, more evidently, vertical deviations. Such deviations are easily detected by the conformance monitor. Figure 4 shows the intruder position and velocity deviations from the actual trajectory to the nominal trajectory. The red dashed lines are the different thresholds, which define replan triggers. In this example, the first replan triggers at $t = 53s$, both due to the vertical position and vertical speed components (blue line). Subsequent predictions (dark orange, yellow, purple and green) are triggered due to the deviations on the vertical

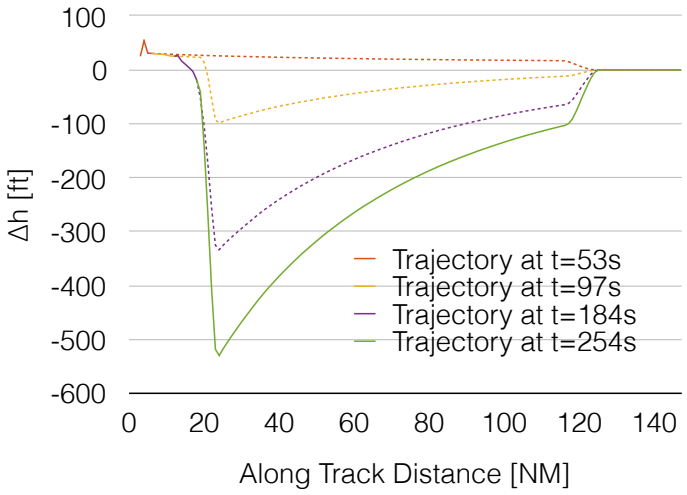


**Fig. 5 Vertical deviation from the initial plan performed by the ownship at each replan in order to deviate from the updated predicted intruder trajectory.**

position component only. This is only due to the specific depicted example, and other cases could be sought that triggered replans due to deviations in any of the other state variables.

With the objective of maintaining separation from the intruder after each new prediction, the ownship generates new trajectories that deviate from the initial plan as the predicted conflict evolves. In this specific case study, even if the optimiser is given flexibility to deviate both horizontally and vertically, the conflict is resolved with deviations on the vertical profile only: both aircraft are climbing and minor changes in the vertical profile give the required vertical separation throughout the flight, having a negligible impact on the fuel consumption. Figure 5 shows this vertical deviation for the different replans (the solid line represents the trajectory that is effectively flown by the ownship, whereas the dashed line depicts what it would have flown if no new replan had been triggered). It is clear how each replan activity creates greater vertical corrective actions and at an earlier time (the initial plan is actually unaware of the conflict due to the prediction errors). See for instance how replan at $t = 184s$ starts deviating earlier than replan at $t = 97s$.

Effectively, figure 6(a) shows the vertical separation between the ownship and the intruder's predicted trajectory, depicting that the minimum separation is always respected from the optimiser's perspective. However, in reality this would not be the case, as presented in figure 6(b), due to the errors in the predictions. Furthermore, even if the vertical separation between both aircraft at the

loss of horizontal separation is increased at every replan, it never reaches the required 1000ft in the presented case. This is explained by the fact that the last replan happens at $t = 254s$, some $50s$ ahead of the conflict, which is enough time for the prediction to grow some error but without triggering a replan (the vertical threshold in the conformance monitoring is set to 250ft). This issue could easily be overcome in any case by increasing the required vertical separation at the optimisation procedure with a buffer accounting for the conformance monitor threshold plus other uncertainty sources. Indeed, figure 7 shows how the conflict is finally removed when the ownship optimisation algorithm takes into account the conformance monitoring threshold (other uncertainty sources are here ignored).

This specific study case presents a conflicting situation that is finally resolved after triggering four replans and only around 70ft extra at the minimum vertical separation between both aircraft. Furthermore, the increase in fuel of the resulting ownship flight when compared to the optimal baseline is negligible (less than 0.004%). Even if these results hint a good performance of the algorithm, future work should be devoted to provide a sensitivity study with many conflict geometries and study cases. This would provide a better understanding of the efficiency of the conformance monitoring framework and the proposed thresholds (quantifiable mainly through the number of replans and the extra fuel burned due to the presumably increased separation at the moment of encounter).

Besides, the conformance monitor could have an adaptive threshold which would decrease as the two aircraft get closer. Additionally, a mass estimation algorithm such as the one described in [40] could be run at each replan to learn from the intruder's past states and produce more accurate predictions, resulting in earlier and more efficient corrective actions.

The application of the described methodology in the example results in an evident enhancement of the conflict resolution. Without it, the ownship would most probably have disregarded the intruder as a potential conflict, due to the big errors in the initial prediction. Thanks to the conformance monitoring, as the flight progresses, the ownship is more and more aware of the conflict and has more time to react. Therefore, the resulting trajectory amendment to avoid the conflict is not only more robust to intruder prediction uncertainties but also more efficient than ATC path stretching or level-offs (as typical tactical interventions to maintain safety), since is the outcome

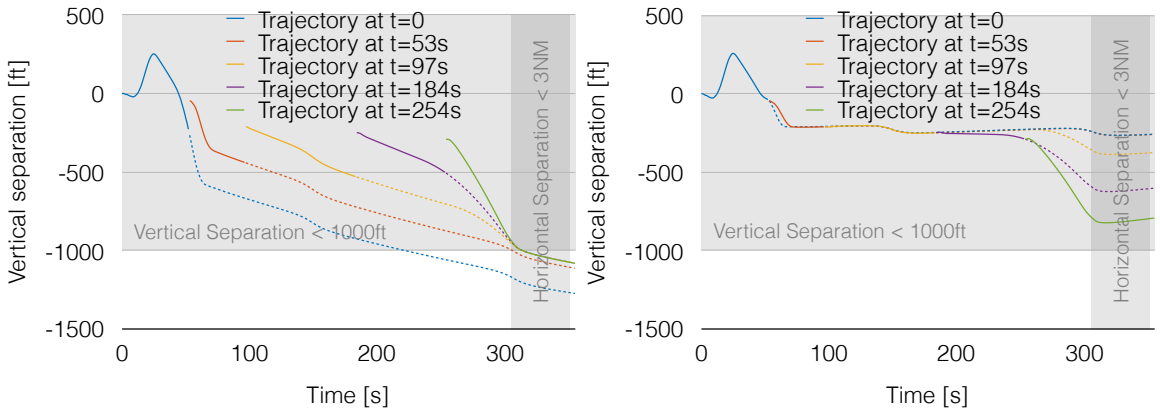


(a) Predicted Separation

(b) Real Separation

**Fig. 6 Vertical separation between the ownship and the intruder.**

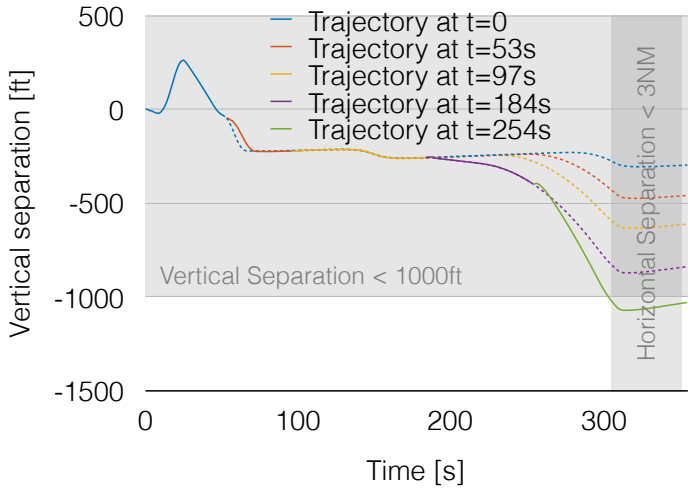


**Fig. 7 Vertical separation between the ownship and the intruder's real trajectory with a required minimum vertical separation of 1250ft.**

of a trajectory optimisation process of the ownship. However, due to the latent errors in the prediction model, the intruder's future states quickly deviate from the reality, and therefore the conflict resolution strategy, even if correctly progressing towards the ultimate removal of it, will not do so until the very last moment, in which case it might be too late (e.g., corrective manoeuvre too aggressive due to lack of earlier action).

## VI. Conclusion and further work

In this paper we have described a framework for optimising 4D trajectories, while maintaining separation to other traffic. Given the fact that trajectory estimates of intruding traffic can be

very inaccurate, techniques for target tracking and conformance monitoring have been introduced. Hence, replans occur either when new information arrives, or when the tracker alerts of a deviation from the expected trajectory. We have described the functional modules and data sharing for an implementation of a semi-cooperative scenario. However, other cooperative cases could easily be integrated in the model: in the case of full cooperation both aircraft would compute own deviations and would agree on the final manoeuvre, given a set of comparable variables, such as consumed fuel, the resulting time of arrival, etc. as the authors presented in Ref. [5]; whereas in the non-cooperative case the trajectory prediction could only rely on current and historical data to produce the immediate future states (these cases will be further studied in future work). Additionally, even if only one conflict is assumed in the results, the implemented separation strategy is easily extrapolated to multiple conflicts. Finally, we have presented a realistic example based on an operational scenario.

In the depicted case, thanks to the conformance monitoring, the different replans reveal an initially unexpected conflict. Effectively, the target tracker could be enhanced to propose modifications to the prediction assumptions. In this case, and since we can easily spot that the predictor is always overestimating the altitude, the expected mass of the aircraft could be slightly increased at each replan. Therefore, assumptions for mass and cost index strategies could be corrected using ADS-B historical data, as the authors presented in Ref. [40]. Besides, given the flexibility with which the scenarios can be defined in our tool, it could easily be extended to a wide variety of scenarios. These scenarios could involve the use of incorrect performance parameters in the predictor, in-air flight plan changes, weather divergences, non conformance to flight plan of non-cooperative aircraft, etc. In future work, an exhaustive set of tests will be defined to demonstrate the performance of the proposed methodology in a sensibility study. Additionally, the conformance monitoring could be extended to propose enhancements to the prediction models as the Kalman filter learns.

The conflict-free optimisation and conformance monitoring algorithms described in this paper are laying out the basis for an interactive all-autonomous air traffic management framework. In a future situation, we could assume that tactical coordination between aircraft (i.e., who should deviate?) will be in place, beyond the collision avoidance currently already implemented through TCAS. Within this paper we provide the tools to resolve the conflict from one of the parts (the

ownship), once the coordination between the aircraft has been agreed. In a highly automated air traffic system the framework described in this paper enhances the situational awareness of the airspace user by providing information of the ownship energy state in accordance to the separation with the surrounding traffic. The methodology is well aligned with SESAR concepts and works towards the enablement of TBO and self-separation.

**Acknowledgments**

The authors would like to thank Airbus Industrie for the use of PEP (Performance Engineers Program) suite, which allowed us to undertake realistic aircraft performance simulations.This work is partially sponsored by SESAR WP-E HALA! Research Network.

**References**

[1] Johnson, C. M., "Analysis of Top of Descent (TOD) Uncertainty," *Digital Avionics Systems Conference (DASC), 2011 IEEE/AIAA 30th*, IEEE, 2011, pp. 1–10.

[2] Soler, M., Kamgarpour, M., and Lygeros, J., "A Numerical Framework and Benchmark Case study for Muti-modal Fuel Efficient Aircraft Conflict Avoidance," *6th International Conference on Research in Air Transportation (ICRAT)*, 2014.

[3] Bronsvoort, J., *Contributions to Trajectory Prediction Theory and its application to arrival management for Air Traffic Control*, Ph.D. thesis, Universidad Politécnica de Madrid, 2014.

[4] De Jong, P. M. A., *Continuous Descent Operations using Energy Principles*, Ph.D. thesis, TU Delft, 2014.

[5] Vilardaga, S. and Prats, X., "Operating cost sensitivity to required time of arrival commands to ensure separation in optimal aircraft 4D trajectories," *Transportation Research Part C: Emerging Technologies*, Vol. 61, 2015, pp. 75–86.

[6] Roy, K., Levy, B., and Tomlin, C., "Target tracking and estimated time of arrival (ETA) prediction for arrival aircraft," *... of AIAA Guidance, Navigation, and Control ...*, , No. August, 2006, pp. 1–22.

[7] Tadema, J., Goossens, A., and Theunissen, E., "Applying NEC to UAS Operations Using an Evolutionary Approach," *15th International Command and Control Research and Technology Symposium, Command and Control Research Program (CCRP)*, 2010.

[8] Blom, H. and Bakker, G. J. B., "Safety of advanced airborne self separation under very high en-route traffic demand," *SESAR Innovation Days*, No. December, 2011, pp. 1–9.

[9] Chaloulos, G., Roussos, G., Lygeros, J., and Kyriakopoulos, K., "Ground Assisted Conflict Resolution in Self-Separation Airspace," *AIAA Guidance, Navigation and Control Conference and Exhibit*, Guidance, Navigation, and Control and Co-located Conferences, American Institute of Aeronautics and Astronautics, aug 2008.

[10] Yang, L., Qi, J., Xiao, J., and Yong, X., "A literature review of UAV 3D path planning," *Intelligent Control and Automation (WCICA), 2014 11th World Congress on*, jun 2014, pp. 2376–2381.

[11] Ruiz, S., Piera, M. a., Nosedal, J., and Ranieri, A., "Strategic de-confliction in the presence of a large number of 4D trajectories using a causal modeling approach," *Transportation Research Part C: Emerging Technologies*, Vol. 39, 2014, pp. 129–147.

[12] Betts, J. T., *Practical methods for optimal control and estimation using nonlinear programming*, No. 19 in Advances in design and control, Society for Industrial and Applied Mathematics, 2nd ed., 2010.

[13] Prats, X., Puig, V., and Quevedo, J., "A multi-objective optimization strategy for designing aircraft noise abatement procedures. Case study at Girona airport," *Transportation Research Part D: Transport and Environment*, Vol. 16, No. 1, jan 2011, pp. 31–41.

[14] Franco, A. and Rivas, D., "Analysis of optimal aircraft cruise with fixed arrival time including wind effects," *Aerospace Science and Technology*, Vol. 32, No. 1, 2014, pp. 212–222.

[15] Visser, H. G. and Hartjes, S., "Economic and environmental optimization of flight trajectories connecting a city-pair," *Proceedings of the Institution of Mechanical Engineers, Part G: Journal of Aerospace Engineering*, Vol. 228, No. 6, 2014, pp. 980–993.

[16] Musialek, B., Munafo, C., Ryan, H., and Paglione, M., "Literature Survey of Trajectory Predictor Technology," Tech. rep., Federal Aviation Administration, William J. Hughes Technical Center, 2010.

[17] Krozel, J., Andrisani, D., Ayoubi, M. A., Hoshizaki, T., Schwalm, C., Conformance, G., Factor, C., Mile, N., Performance, R. N., Radar, S. S., Alert, T., Change, T., Point, T. C., Introduction, I., Scientist, C., Division, D., Researcher, P.-d., and Analyst, S., "Aircraft ADS-B Data Integrity Check," 2004, pp. 1–11.

[18] Reynolds, T. G. and Hansman, R. J., "Investigating Conformance Monitoring Issues in Air Traffic Control Using Fault Detection Techniques," *Journal of Aircraft*, Vol. 42, No. 5, sep 2005, pp. 1307–1317.

[19] Seah, C. E., Aligawesa, A., and Hwang, I., "Algorithm for Conformance Monitoring in Air Traffic Control," *Journal of Guidance, Control, and Dynamics*, Vol. 33, No. 2, mar 2010, pp. 500–509.

[20] Chong, R. S., "Assessing the operational benefits of Automated Conformance Monitor for RNP-to-Final operations," *2012 IEEE/AIAA 31st Digital Avionics Systems Conference (DASC)*, oct 2012, pp.

4D5–1–4D5–12.

[21] Sotiriou, D., Kopsaftopoulos, F., and Fassois, S., "An Adaptive Time-Series Probabilistic Framework for 4-D Trajectory Conformance Monitoring," *IEEE Transactions on Intelligent Transportation Systems*, Vol. 17, No. 6, jun 2016, pp. 1606–1616.

[22] Eurocontrol, "Review of ASAS Applications studied in Europe," Technical report, CARE/ASAS Action. CARE/ASAS Activity 4, 2002.

[23] Gallo, E., López-Leonés, J., Vilaplana, M. Á., Navarro, F., and Nuic, A., "Trajectory computation Infrastructure based on BADA Aircraft Performance Model," *2007 IEEE/AIAA 26th Digital Avionics Systems Conference*, 2007.

[24] SESAR, "Sistem Wide Information Management. ATM Information Reference Model," Tech. rep., SESAR, 2012.

[25] Bezawada, R., Duan, P., and Uijt de Haag, M., "Hazard tracking with integrity for surveillance applications," *Digital Avionics Systems Conference (DASC), 2011 IEEE/AIAA 30th*, oct 2011, pp. 8C1–1–8C1–15.

[26] Prats, X., *Contributions to the optimisation of aircraft noise abatement procedures*, Ph.D. thesis, Universitat Politècnica de Catalunya, 2010.

[27] Betts, J. T. and Cramer, E. J., "Application of Direct Transcription to Commercial Aircraft Trajectory Optimization," *Journal of Guidance, Control and Dynamics*, Vol. 18, No. 1, 1995, pp. 151–159.

[28] RTCA SC-186, "Minimum Operational Performance Standards (MOPS) for 1090 MHz Extended Squitter Automatic Dependent Surveillance-Broadcast (ADS-B) and Traffic Information Services-Broadcast (TIS-B)," 2009.

[29] Gong, C. and Sadovsky, A., "A Final Approach Trajectory Model for Current Operations," *10th AIAA Aviation Technology, Integration, and Operations (ATIO) Conference*, American Institute of Aeronautics and Astronautics, Reston, Virigina, sep 2010.

[30] ICAO, "Procedures for Air Navigation Services. Air Traffic Management," Tech. rep., 14th ed., International Civil Aviation Organisation, doc. 4444, Montreal (Canada), 2001.

[31] Raghunathan, A. U., Gopal, V., Subramanian, D., Biegler, L. T., and Samad, T., "Dynamic optimization strategies for three-dimensional conflict resolution of multiple aircraft," *Journal of guidance, control, and dynamics*, Vol. 27, No. 4, 2004, pp. 586–594.

[32] Mohan, K., Patterson, M., and Rao, A. V., "Optimal Trajectory and Control Generation for Landing of Multiple Aircraft in the Presence of Obstacles," *Guidance, Navigation, and Control Conference*, No. August, American Institute of Aeronautics and Astronautics, Minneapolis, Minnesota, 2012, pp. 1–16.

[33] Menon, P. K., Sweriduk, G. D., and Sridhar, B., "Optimal Strategies for Free Flight Air Traffic Conflict Resolution," *Journal of Guidance, Control and Dynamics*, 1997, pp. 1–35.

[34] Brown, R. and Hwang, P. Y. C., *Introduction to Random Signals and Applied Kalman Filtering*, New York, 1997.

[35] Aeropuertos Españoles y Navegación Aérea, "Normalised Departure Chart. Standard Instrumental Procedure for Barcelona / El Prat. RWY25L / RWY20," 2012.

[36] Aeropuertos Españoles y Navegación Aérea, "Normalised Departure Chart. Standard Instrumental Procedure for Reus. RWY07," 2010.

[37] RTCA SC-181, "Minimum Operational Performance Standards for Required Navigation Performance for Area Navigation," 2003.

[38] RTCA SC-181, "Minimum Aviation System Performance Standards: Required Navigation Performance for Area Navigation," 2003.

[39] RTCA SC-186, "Minimum Aviation System Performance Standards for Automatic Dependent Surveillance-Broadcast (ADS-B)," 2002.

[40] Vilardaga, S. and Prats, X., "Mass Estimation for an Adaptive Trajectory Predictor using Optimal Control," *5th International Conference on Application and Theory of Automation in Command and Control Systems (ATACCS)*, 2015.